Isomerism and Novel Magnetic Order in Mn₁₃ Cluster

S. K. Nayak*,† and M. Nooijen*

*Princeton Materials Institute and Department of Chemistry, Princeton University,
Princeton, New Jersey 08544*

P. Jena

Department of Physics, Virginia Commonwealth University, Richmond, Virginia 23284-2000

Received: July 26, 1999

First principles calculations based on the generalized gradient approximation to the density functional theory reveal the existence of two nearly degenerate isomeric forms of Mn_{13} cluster. The lowest energy structure corresponds to icosahedric packing that lies 0.65 eV lower than a caged structure with a hexagonal close-packed motif. Magnetically, however, these two isomers are very different: while the icosahedric structure is ferrimagnetic with a total magnetic moment of 33 μ_B, the hexagonal close-packed structure is a de facto antiferromagnet with a magnetic moment of 17 μ_B. The two isomers also have different ionization potentials, 5.19 and 4.82 eV, in good agreement with experiment.

Manganese is a unique element in the 3d-transition metal series. With a $3d^5 4s^2$ atomic configuration, it shares properties that are common to both alkaline-earth and transition metals. The filled s-configuration of manganese atoms prevents them from interacting strongly with each other, and as a consequence small clusters of Mn are expected to be bound weakly by van der Waal's type coupling as in Mg and Hg clusters. The unfilled quasi-localized d-electrons of Mn atom, on the other hand, are responsible for its sizable magnetic moment (5 μ_B/atom) while the Hg atom, for example, due to its filled d shell, carries no moment. Thus, the magnetic interaction between Mn atoms as they agglomerate is expected to lend its cluster different properties than Hg clusters.

A few years ago,[1] single-photon ionization thresholds of mercury clusters up to 70 atoms showed a sharp decrease in ionization potential ~2 eV between Hg_8 and Hg_N, $N \leq 35$. This size dependence was attributed to a nonmetal to metal transition in Hg_N clusters where the bonding changes from van der Waal's in small clusters to metallic in large clusters. Recently Koretsky and Knickelbein,[2] following the experimental technique of Parks et al.,[3] studied the ionization potential of Mn_N clusters in the size range $7 \leq N \leq 64$. They found no signature of a nonmetal to metal transition behavior in this size range as the Mn_N ionization potential did not resemble that of Hg_N clusters.[1] In contrast, Parks et al.[3] had earlier observed the onset of reactivity of Mn_N to hydrogen at $N = 16$ and attributed this effect to be due to a nonmetal to metal transition. Failure by Koretsky and Knickelbein[2] to observe any anomaly in the ionization potential (IP) at Mn_{16} casts doubt on the suggestion of Parks et al.[3]

Koretsky and Knickelbein,[2] however, noticed that the IP's of manganese clusters with $N = 7$, 13, and 19 are higher than those of neighboring sizes. They have suggested that these local maxima may be due to compact geometric structures with an icosahedric packing sequence—the 7-atom cluster with a pentagonal bipyramid structure, the 13-atom having an icosahedric structure with its first atomic shell closed, and the 19-

atom cluster adopting a "double" icosahedron structure. In addition to these local maxima in the IP's, the authors also observed the presence of a noticeable break in the photoionization efficiency spectrum in Mn_{13}. They concluded that, in analogy with similar observation in $Nb_{9,11,12}$[4] and Ta_{12} clusters,[5] this could be due to the presence of isomers of the Mn_{13} cluster. They found no such anomalies in the IP's of other Mn clusters studied and were unable to predict definitive structural assignments of Mn_{13} isomers. They concluded by noting that the structures of the isomers await quantum chemical calculations. In this paper, such calculations are presented for the first time.

We have used the molecular orbital approach where the cluster wave function is expressed in terms of a linear combination of atomic orbitals centered at individual atomic sites. The atomic orbitals were represented by a double numerical basis including polarization functions. The coefficients of linear combination were determined self-consistently by solving the density functional equations within the generalized gradient approximation.[6] The geometry and spin optimization as well as binding energy calculations were carried out using the DMOL software.[7] The accuracy of this procedure has been tested earlier by comparing the results with those calculated using the Gaussian 94 code for small manganese clusters as well as with experiment.[8]

It is important to address here the concern regarding spin contamination and broken symmetry solutions in DFT calculations. Within the DFT framework the calculation of S_z is well-defined, as it can be obtained from the spin density. The calculation of S^2 is much more cumbersome since it is a two-electron operator that cannot be obtained as an expectation value of the spin-polarized density. Within the DFT framework, one possible rigorous approach requires that S^2 is added as a perturbation to the Hamiltonian, and the expectation value of S^2 is calculated as a response property. This has never been tried to the best of our knowledge, as it would require construction of a functional that is sensitive to a completely different Hamiltonian (functionals are universal only insofar as they correspond to electrons interacting through Coulombic

---

† Princeton Material Institute fellow.

forces). An alternative treatment is based on the fact that S^2 can be obtained from knowledge of the spin-dependent density and the spin-dependent correlation holes.[9] The correlation holes can be modeled in terms of the density and this provides a route to calculate S^2 within a DFT conceptual framework.[9] The most common way to calculate S^2 is that the single determinantal Kohn−Sham wave function is interpreted as a genuine wave function and S^2 is calculated as an expectation value of the KS wave function.[10−11] This value of S^2 corresponds to the easily computable S^2 value of the noninteracting system that has the same spin-density as the true system. In the past[12,13] it has been found that for high-spin systems ($S = S_z$) that can be described as a single determinant, spin contamination as found from an unrestricted Kohn−Sham wave function is typically very minor. However, the Mn_{13} cluster considered here does not fall into this class at all. If S^2 is calculated from the KS determinant spin contamination is very strong. However, it is far from clear if this evaluation of S^2 is appropriate for such a system. If the exact KS functionals (for energies *and* S^2) were known, all would be fine even if the exact KS determinant would be spin-contaminated.[14] For this reason, we choose not to use spin-projection techniques (based on determinantal based S^2 values). In fact, recent studies have advised against the use of spin projection in DFT to improve the result.[12−13] The issue is controversial and rigorous quantum chemical calculations on small systems might shed more light on the problem. Recent work has discussed the possibilty of canted spins within a DFT framework. This provides yet another mechanism to break symmetry and hence lower the energy.[15] The physical origin of such calculation is not clear, however. In this work we assume that the energetics and density is calculated appropriately from unrestricted KS theory using the GGA approximation, even for systems for which the true wave function cannot at all be described by a single determinant. In DMOL the energy is optimized over all spin densities that have integer values for S_z. The calculated optimal value of S_z is a lower bound to S in the ground state, and we interpret the calculated spin-density to correspond to the spin density of the $M_S = S$ state. Clearly in the current state of the art KS density functional theory, these assumptions can be wrong: most notable is the example of broken symmetry antiferromagnetic state corresponding to $S = 0$, which has a spin density that net integrates to zero.[16] This is physically incorrect and is due to the errors in current functionals. In the absence of the perfect functional and the perfect density, as Pople et al. pointed out,[14] comparison of theoretical and experimental properties can provide a simple and direct test of the calculation. Interestingly, many studies[17] have shown that the spin densities computed at the DFT level, in general, are in good agreement with those obtained from experiment including those obtained from broken symmetry calculations. In addition, density functional theory within the generalized gradient approximation has correctly predicted the magnetic structure of many systems including a Rh surface which has been recently studied,[18] although the energies corresponding to magnetic and nonmagnetic solutions are very close. This prediction has been recently verified by experiment.[19] Perdew et al.[20] have recently critically examined density functional theory and its applications to magnetism in various systems such as ferromagnetic solids (Fe, Co, Ni) as well as antiferromagnetic systems (FeO solid, Cr_2). Their study shows that the energetics of both ferromagnetic and antiferromagnetic systems are reliable. They have further shown that the spin densities break the symmetry (i.e., evidently do not correspond to pure spin states) in systems such as in Cr_2 in order to give the correct energies.
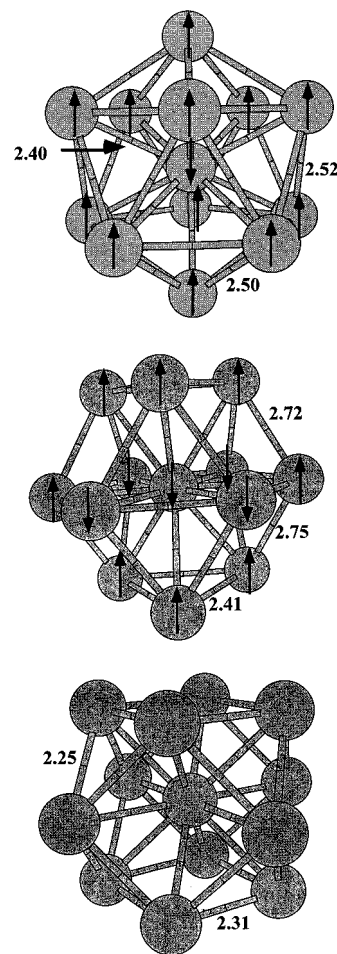
Figure 1. Optimized geometries of Mn_{13} isomers: (a, top) icosahedric and (b, middle) hcp structures are nearly degenerate while the (c, bottom) cuboctahedric structure lies 0.4 eV/atom above the ground state.

The spin densities themselves are trustworthy only in ferromagnetic systems and should be taken with caution in antiferromagnetic systems.[20]

It is well-known that the potential energy surface of a cluster can be plagued with a multitude of local minima and, during geometry optimization, the system can be trapped in one of these local minima. We have, therefore, used three different initial starting configurations: clusters having icosahedric, hexagonal close-packed, and cuboctahedric structures. These starting configurations are slightly distorted from their higher symmetry structures and the geometry optimization is carried out by following the method of steepest descent. This requires $3N - 6 = 33$ geometrical parameters to be varied independently and simultaneously. The removal of any symmetry constraint in the calculation (i.e., broken symmetry calculation) allows the possibility of both ferromagnetic and antiferromagnetic alignment in the cluster. This is important as Mn atoms are expected to carry sizable magnetic moments, but their ordering a priori is not known. For example, the α-phase of bulk manganese is antiferromagnetic while very small clusters are ferromagnetic.[8,21] It is not clear how the transition from ferromagnetic to antiferromagnetic order would occur in these clusters as a function of cluster size.

In Figure 1 we give the various optimized geometries of Mn_{13} clusters. The distance between the atoms in these clusters lie between the dimer bond distance (3.5 Å)[8] and the bulk interatomic distance (2.29 Å).[22] The decrease in the bond distance with the increase in cluster size is a signature of increase

TABLE 1: Binding Energy per Atom, Vertical Ionization Potential, and Magnetic Moment per Atom of Mn$_{13}$ Isomers

cluster	BE (eV)	IP (eV)	magnetic moment (μ_B)
Figure 1a icosahedric	1.77	5.19	2.54
Figure 1b hcp	1.72	4.82	1.31
Figure 1c cuboctahedric	1.33	5.30	0.39

in bonding in Mn cluster.[8] Although the structures are distorted from the perfect icosahedric, hexagonal-closed packed (hcp), and cuboctahedric geometries, their resemblance to their packings can be clearly seen. Vibrational frequencies are computed for these two geometries and the structures are found to be minima in the potential energy surface. The corresponding binding energy/atom, vertical ionization potential, and magnetic moment/atom of these isomers are given in Table 1. We note that energetically the icosahedric geometry is the most preferred structure. The hcp structure, the next higher energy isomer, lies 0.65 eV above the ground state. The presence of higher energy isomers in the gas phase is well-known[23] and the hcp structure could exist in the beam simultaneously. It will be interesting to carry out similar experiments under different conditions (e.g., varying the temperature) in order to isolate the different isomers. The cluster mimicking the cuboctahedric structure is significantly higher in energy, namely 5.2 eV, and is not likely to be present.

The ionization potentials are calculated by taking the difference in the total energies of the neutral and singly positively charged cluster at the neutral geometry. The isomer with the icosahedric structure has an ionization potential of 5.19 eV while the hcp structure's IP is 4.82 eV. The experimental values are 5.30 and 4.80 eV.[2] This good agreement with experiment suggests that we have correctly identified the geometries of the Mn$_{13}$ isomers.

The difference in the magnetic property of these isomers is interesting: First, the total magnetic moment of the icosahedric structure is 33 μ_B while that of the hcp structure is 17 μ_B. Second, the alignment of the moments in these isomers is very different. In the icosahedric isomer, the outer shell of atoms have their magnetic moments aligned in the parallel direction and each carry a moment of 2.91 μ_B. These are coupled antiferromagnetically to the moment at the central site which has a value of -1.89 μ_B. This ferrimagnetic coupling sharply contrasts with the ferromagnetic coupling in very small clusters where the magnetic moment/atom is 5 μ_B and anti-ferromagnetic coupling in the α-phase of bulk Mn.[24] Although no direct measurements of the magnetic moment/atom in bulk Mn are available, it is believed to be around 3 μ_B/atom.[24] Thus, while the magnetic moment/atom in Mn$_{13}$ appears to be bulklike, the magnetic coupling proceeds from ferro- to ferri- to antiferromagnetic as cluster size increases.

The caged hcp isomer, on the other hand, has a much smaller magnetic moment than the icosahedric structure. The average magnetic moment/atom is only 1.31 μ_B. This small value results from a substantial cancellation between up and down moments. Here, there are eight atoms that have moments pointing up while five atoms have moments pointing down. We term this arrangement as a de facto antiferromagnet. Note that the Mn$_{13}$ cluster, because of its odd number of atoms, will always carry a net moment irrespective of its magnetic ordering since its half-filled d-shells renders each atom with a moment. What is interesting in the magnetism of the hcp structure (Figure 1b) is the coupling. We can divide this structure into three planes: the top and bottom planes containing three atoms each and the
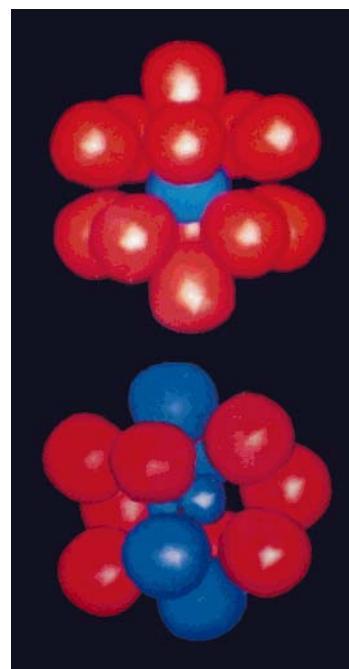
Figure 2. Plot of the spin density distribution in (a, top) icosahedric and (b, bottom) hcp structure of Mn$_{13}$ isomers. The red color indicates positive (↑) while the blue color indicates negative (↓) spin densities.

central plane containing seven atoms with the outer six forming a hexagon and the seventh atom occupying the central site. The total net moments of the top and bottom planes are 11.45 μ_B each pointing up. The moment of the central atom points down, but its magnitude is considerably less, namely 0.8 μ_B. Among the six atoms forming the hexagon in the middle plane, four have moments pointing down in the range between 3.15 and 2.5 μ_B while the other two have moments pointing up, 2.94 μ_B each (see Figure 1). The cuboctahedric structure that is energetically higher has even less moment, namely 0.39 μ_B/atom.

The distribution of moments at different atomic sites can be seen by plotting the spin densities. In Figure 2 we plot these distributions for the two nearly degenerate isomers (Figure 1a,b). These are consistent with the direction of the moments deduced from the Mulliken analysis and given in Figure 1. The substantial dependence of the magnetic character of clusters on structure is characteristic of what is known in bulk manganese which has many allotropic forms with widely different magnetic properties. Unfortunately, no experiments on the magnetic properties of Mn clusters in the gas phase are yet available. The fact that the calculated ionization potentials of Mn$_{13}$ isomers agree well with experiment should lend credibility to our prediction concerning its novel magnetic properties. Clearly the rich variety of magnetic behavior of Mn$_{13}$ cluster isomers alone suggests that these experiments should be performed.

It will also be interesting to study the reactivity of Mn$_{13}$ cluster isomers with reagent molecules such as H$_2$ and O$_2$. We have demonstrated earlier[18] that Rh$_4$ cluster isomers, which have different magnetic properties, react with H$_2$ differently: The nonmagnetic Rh$_4$ binds more strongly to hydrogen than its magnetic isomer. We note that the ionization potential of the icosahedric structure is larger than the hcp structure. The icosahedric structure also carries a larger magnetic moment than the hcp structure. Thus, larger ionization potential is coupled with larger magnetic moment. Since clusters with larger ionization potential are often less reactive than those with lower

ionization potential, it will be interesting to see if the anomalous reactivity change of Mn$_N$ clusters at $N = 16$ is of magnetic origin. Such a theoretical study is in progress.

References and Notes

(1) Brechignac, C., et al. *Phys. Rev. Lett.* **1988**, *60*, 275. Rademann, K., et al. *Phys. Rev. Lett.* **1987**, *59*, 2319.
(2) Koretsky, G. M.; Knickelbein, M. B. *J. Chem. Phys.* **1997**, *106*, 9810.
(3) Parks, E. K.; Nieman, A. C.; Riley, S. J. *J. Chem. Phys.* **1996**, *104*, 3531.
(4) Knickelbein, M. B.; Yang, S. *J. Chem. Phys.* **1990**, *93*, 5760.
(5) Collings, B. A., et al. *Int. J. Mass Spectrom. Ion Processes* **1993**, *125*, 207.
(6) Becke, A. D. *Phys. Rev. A* **1988**, *38*, 3098. Perdew, J. P.; Wang, Y. *Phys. Rev. B* **1992**, *45*, 13244.
(7) DMOL Code, Biosym Technologies, San Diego, CA.
(8) Nayak, S. K.; Jena, P. *Chem. Phys. Lett.* **1998**, *289*, 473.
(9) Wang, J.; Becke, A.; Smith, V. *J. Chem. Phys.* **1995**, *102*, 3477.
(10) Laming, G. J.; Handy, N. C.; Amos, R. D. *Mol. Phys.* **1993**, *80*, 1121.
(11) Zhao, X.-G. et. al. *Inorg. Chem.* **1997**, *36*, 1198. Rodriguez, J. H.; Wheeler, D. E.; McCusker, J. M. *J. Am. Chem. Soc.* **1998**, *120*, 12051.
(12) Baker, J.; Scheiner, A. Andzelm, J. *Chem. Phys. Lett.* **1993**, *216*, 380.
(13) Wittbrodt, J.; Schlegel, H. B. *J. Chem. Phys.* **1996**, *105*, 6574. Goldstein, E.; Beno, B.; Houk, K. N. *J. Am. Chem. Soc.* **1996**, *118*, 6036.
(14) Pople, J. A.; Gill, P. M. W.; Handy, N. C. *Int. J. Quantum Chem.* **1995**, *56*, 303.
(15) Oda, T.; Pasquarello, A.; Car, R. *Phys. Rev. Lett.* **1998**, *80*, 3622.
(16) Delley, B.; Freeman, A. J.; Ellis, D. E. *Phys. Rev. Lett.* **1983**, *50*, 488.
(17) Zheludev, A., et al. *J. Am. Chem. Soc.* **1994**, *116*, 7243. Baron, et al. *J. Am. Chem. Soc.* **1996**, *118*, 11822.
(18) Nayak, S. K., et al. *Phys Rev B* **1997**, *56*, 8849. Cho, J.-H.; Scheffler, M. *Phys. Rev. Lett.* **1997**, *78*, 1299.
(19) Goldoni, A., et al. *Phys. Rev. Lett.* **1999**, *82*, 3156.
(20) Perdew, J. P., et al. *Int. J. Quantum Chem.* **1997**, *61*, 197.
(21) Pederson, M. R.; Reuse, F.; Khanna, S. N. *Phys. Rev. B* **1998**, *58*, 5632.
(22) Kittel, C. *Introduction to Solid State Physics*; Wiley: New York, 1986.
(23) Nayak, S. K.; Rao, B. K.; Jena, P.; Li, X.; Wang, L. S. *Chem. Phys. Lett.* **1999**, *301*, 379.
(24) Arrot, A. In *Magnetism*; Rado, G. T., Suhl, A., Eds.; Academic Press: New York, 1966; Vol. IIB, p 295.